Early-stage pharmaceutical development of bilayer buccal films with a chitosan backing layer for local pain management in oral mucositis

European Journal of Pharmaceutical Sciences 221 (2026) 107530

Contents lists available at ScienceDirect

European Journal of Pharmaceutical Sciences

journal homepage: www.elsevier.com/locate/ejps

Early-stage pharmaceutical development of bilayer buccal films with a chitosan backing layer for local pain management in oral mucositis

Karin Korelc [a,*], Vishnu Arumughan [b], Åke Henrik-Klemens [c,d], Anette Larsson [c], Ingunn Tho [a]

[a] Department of Pharmacy, University of Oslo, P.O.Box 1068 Blindern, 0316 Oslo, Norway
[b] Dept. of Bioproducts and Biosystems, School of Chemical Engineering, Aalto University, Finland
[c] Dept. of Chemistry and Chemical Engineering, Chalmers University of Technology, Sweden
[d] FibRe Centre for Lignocellulose-Based Thermoplastics, Department of Chemistry and Chemical Engineering, Chalmers University of Technology, Sweden

ARTICLE INFO

Keywords:
Chitosan
HPMC
Local drug delivery
Side-by-side cells
Bilayer films
Buccal films

ABSTRACT

Oral mucositis is a painful inflammation and ulceration of the oral mucosa that frequently occurs as a side effect of radiation and chemotherapy that impairs patients' quality of life, making eating and drinking challenging. Local anesthetics applied directly to lesions can provide temporary pain relief without substantial systemic exposure. Buccal films are a promising delivery platform because they protect the sore area while releasing anesthetics locally to the inflamed mucosa. In this work, the mucoadhesive and swelling properties of chitosan were exploited as a backing layer in bilayer films whose inner drug-loaded layer comprised hydroxypropyl methyl cellulose (HPMC). Formulations containing HPMC of two molecular weights (low and high Mw) at concentrations chosen to give similar viscosity in solution (9% and 2.8% w/w, respectively), were tested with chitosan at 2% and 3% w/w. Interactions between chitosan and HPMC were confirmed by QCM-D. Tetracaine and bupivacaine served as model drugs. Films containing 5–10 mg drug were transparent and non-crystalline; higher drug loads produced crystallization on drying. Drug release was monitored simultaneously from the drug-containing layer and the chitosan backing layer in a side-by-side setup, and the best formulation was able to limit the drug release through the backing layer by about 70% for one hour. This early-stage study shows that chitosan is a promising backing layer for bilayer films, reducing the amount of drug released into the oral cavity. Additionally, it may improve mouthfeel and mucosal residence time while enhancing therapeutic efficacy and patient comfort.

1. Introduction

Oral mucositis is a common chemotherapy- and radiotherapy-induced complication, occurring in between 40 and 80% of patients (Cheng et al., 2001; Kang et al., 2024). Patients suffering from oral mucositis develop erosive and ulcerative lesions and swollen mucosa as a result of epithelial damage, causing intense pain and discomfort. The disease can negatively impact patients' ability to swallow, eat, drink, communicate, and sleep, leading to reduced quality of life, systemic malnutrition and decreased immunity, and, in severe cases, treatment interruption/termination (Kang et al., 2024). The symptoms usually appear a couple of days after chemotherapy initiation and persist for 3 weeks before the homeostasis in the buccal cavity can be reestablished; however, for head and neck cancer patients with generally poorer outcome, the restored stage is often not reached. Regular buccal hygiene is crucial to minimize the severity and duration of mucositis (Alves et al., 2020; Cheng et al., 2001).

The treatment of oral mucositis generally involves the use of anesthetics or analgesics, such as 20 mg/mL lidocaine viscous solution or 0.2% topical morphine rinse for pain management, and most patients additionally receive systemic opioids, which are associated with systemic side effects such as risk of addiction and somnolence (Lalla et al., 2008; Sarvizadeh et al., 2015). Other mucositis treatment strategies involve the incorporation of antifungals, antimicrobials, prostaglandins and radioprotectors (Alves et al., 2020; Cheng et al., 2001).

Local anesthetics reduce pain in the mouth by blocking impulses in peripheral nerves (Ngo et al., 2020). The common local anesthetics for topical application include benzocaine, lidocaine and tetracaine hydrochloride (Tofoli et al., 2025). Tetracaine is an ester-type anesthetic with a rapid onset of action and a long duration (Kaewjiaranai et al.,

* Corresponding author at: Department of Pharmacy, P.O. Box 1068 Blindern, 0316, Oslo, Norway.
E-mail address: karin.korelc@farmasi.uio.no (K. Korelc).

https://doi.org/10.1016/j.ejps.2026.107530
Received 23 January 2026; Received in revised form 1 April 2026; Accepted 14 April 2026
Available online 15 April 2026

2018). Previous attempts to formulate a tetracaine-based oral gel were found effective in reducing oral cavity pain in mucositis patients (Alterio et al., 2006). Bupivacaine is an amide-type anesthetic with a long duration and is suitable to achieve prolonged pain relief (Katzung, 2019; Mogensen et al., 2016; Ngo et al., 2020).

Buccal mucoadhesive films offer easy, painless administration to the oral cavity without having to swallow the film. They are suitable for both local and systemic drug delivery while avoiding first-pass metabolism (Shipp et al., 2022; Smart, 2005). Additionally, they provide a longer residence time on the administration site compared to semi-solid formulations, such as gels and creams, due to their mucoadhesive properties (Tofoli et al., 2025). Mucoadhesive buccal films usually consist of hydrophilic polymers that hydrate and form hydrogel upon contact with the saliva (Smart, 2005). The swollen hydrogel can additionally protect the ulcerative lesions from outside factors.

Application of the films with a local anesthetic to the buccal mucosa may result in both local and systemic effects. To maximize the unidirectional delivery of a drug to the painful area, an additional backing layer can be added to the film (i.e., bilayer film) to reduce the amount of drug being released into the oral cavity. Commonly proposed backing layers in the literature consist of an insoluble polymer, such as ethyl cellulose (EC), melted wax or plastic patch material (Preis et al., 2014). However, for oral mucositis patients, it could be beneficial to have a backing layer that offers additional functionalities, such as creating a soft gel-like surface to improve the mouthfeel and mucoadhesive properties for prolonged residence time on the mucosa.

Chitosan (CHIT) is a natural cationic polysaccharide, obtained by chitin deacetylation (Szymańska and Winnicka, 2015). It is attractive for drug delivery due to its beneficial properties, such as biocompatibility, biodegradability, and possessing mucoadhesive, antimicrobial and wound-healing properties (Younes and Rinaudo, 2015). Chitosan is hygroscopic, swells and forms hydrogen bonds with water and, when formulated into films, maintains the matrix shape at neutral pH (Korelc et al., 2023). For these reasons, it can be applied as a potential backing layer in film formulations with the aim of reducing the amount of drug released through the chitosan layer, while improving the mouthfeel and physically protecting the damaged area.

Hydroxypropyl methyl cellulose (HPMC) is a cellulose derivative, often used in pharmaceutics because of its non-toxicity, availability, biodegradability and water-solubility, making it suitable for drug release rate control (Fahs et al., 2010; Ghadermazi et al., 2019; Kamel et al., 2008). In HPMC-based matrices, the drug release is governed by HPMC hydration and swelling (and thereby drug diffusion through the swollen gel layer), and by the erosion rate of the swollen layer, which generally decreases with increasing molecular weight (Kamel et al., 2008). HPMC is a suitable agent for film preparation, and the films are generally transparent, flexible and have good mechanical properties (Ghadermazi et al., 2019; Mahadevaiah et al., 2016).

The aim of this project was to explore chitosan as a backing layer for bilayer buccal films with local anesthetics, bupivacaine (BPA) and tetracaine (TCA), using HPMC as a drug-containing layer. Such films could be beneficial to provide pain relief for patients with oral mucositis. The study focused on early-stage pharmaceutical development of the films to identify parameters relevant for preparation of bilayer films. Chitosan layer should hinder the amount of drug released into the oral cavity and thereby reduce systemic circulation, as well as improve the mouthfeel and provide an additional wound-healing and antimicrobial effect. Two types of HPMC, low and high molecular weight (Mw), in concentrations selected to give similar viscosity in water, were used as the drug containing layer. Two concentrations of the chitosan were tested as backing layer to investigate the thickness of the chitosan layer necessary to limit the drug release through the backing layer.

2. Materials and methods

2.1. Materials

Bupivacaine hydrochloride monohydrate (BPA) was obtained from Sigma Aldrich. Tetracaine hydrochloride (TCA) was obtained through Apotekproduksjon AS, Norway. HPMC 4000 with high Mw (HPMC HM) (viscosity 4460 cP, 2% in H_2O at 20 °C) was purchased from Fagron, Denmark. Hydroxypropyl methylcellulose with low Mw (HPMC LM) (viscosity 40–60 cP, 2% in H_2O at 20 °C), lactic acid, ethyl cellulose (EC), and phosphate buffer saline (PBS) tablets were obtained from Sigma Aldrich (St. Louis, MO, USA). Chitosan of the ultrapure pharmaceutical grade "Chitopharm™ CM" (98% degree of deacetylation, molecular weight not specified) was provided by Chitinor, Norway.

2.2. QCM-D

Quartz crystal microbalance with dissipation (QCM-D) was used to study the interaction between chitosan and HPMC, both low and high molecular weight. The interaction between the two layers was determined using the QCM-D instrument from Biolin scientific, Sweden, according to (Arumughan et al., 2026). Briefly, chitosan films were prepared on a cleaned SiO_2-coated QCM-D sensor. The films were prepared by dissolving 1% w/w chitosan in 1% v/v acetic acid. The solution was filtered through a 0.2 μm syringe filter to remove undissolved polymer, and 150 μL was spin-coated onto a sensor at 5000 rpm for 60 s with an acceleration of 2500 rpm/min. The film was stabilized and neutralized in 0.5 M NaOH solution for 10 min, rinsed with water, and stored in a desiccator until use. Homogeneity and morphology of the film were investigated by atomic force microscopy (AFM) (INTEGRA Prima setup NT-MDT Spectrum Instruments, Russia). A HPMC solution was prepared by dissolving HPMC in distilled water to obtain the final concentration of 0.1% w/w. The QCM-D experiment was performed by recording the baseline for the film with water, followed by rinsing the sensor with the HPMC solution in water for 60 min, and rinsing the sensor again with water. The recorded frequency at this point referred to the irreversibly attached HPMC. The amount of adsorbed HPMC was calculated using Johannsmann's model (Johannsmann, 2008). Four replicates were performed for each combination.

2.3. Wet polymer solution preparation and formulations

The drug-containing solutions were prepared by first dissolving the drug in water to obtain 10 mg/g and 20 mg/g solutions. The polymer concentration selected to obtain solutions of similar viscosities of the two HPMC types (9% w/w HPMC LM or 2.8% w/w HPMC HM) was added and left to disperse in the drug solution overnight to obtain a homogeneous polymer solution. A chitosan solution was prepared by dispersing chitosan in lactic acid, and the mixture was stirred overnight to obtain a transparent dispersion. 1% and 1.5% v/v lactic acid (pH 2.08 and 1.93, respectively) were used to dissolve 2% and 3% w/w chitosan, respectively. A list of developed and tested formulations is shown in Table 1. Films with ethyl cellulose (EC) were prepared as a reference with an insoluble backing layer for release studies. 8% w/w EC was dissolved in 96% ethanol. Furthermore, placebo films without the drug were produced to evaluate the impact of polymer concentration on disintegration. Placebo chitosan/HPMC LM and chitosan/HPMC HM films were prepared at both concentrations (2.8% and 9%) to match the polymer concentrations used in the corresponding film formulations (see Table 1). Due to the high viscosity of HPMC HM, it was not possible to prepare a 9% solution. Therefore, to prepare a film corresponding to 9% w/w HPMC HM, a 3% w/w HPMC HM solution was prepared, and deposited onto the chitosan films three times to obtain the same thickness.

Table 1
Composition of film formulations and drug proportion in the dry drug film layer, calculated as weight(drug)/weight(drug+polymer).

Formulation	Drug loading (mg)		HPMC layer (% w/w)		Backing layer (% w/w)		Drug proportion
	BPA	TCA	LM	HM	CHIT	EC	
B1	5	-	9	-	2	-	0.10
B2	10	-	9	-	2	-	0.26
B3	5	-	-	2.8	2	-	0.18
B4	10	-	-	2.8	2	-	0.42
B5	5	-	9	-	3	-	0.18
B6	10	-	9	-	3	-	0.10
B7	5	-	-	2.8	3	-	0.42
B8	10	-	-	2.8	3	-	0.26
T1	-	5	9	-	3	-	0.10
T2	-	10	9	-	3	-	0.18
T3	-	5	-	2.8	3	-	0.26
T4	-	10	-	2.8	3	-	0.42
R1*	10	-	9	-	-	8	0.18
R2*	10	-	-	2.8	-	8	0.42
P1**	-	-	2.8	-	3	-	-
P2**	-	-	9	-	3	-	-
P3**	-	-	-	2.8	3	-	-
P4**	-	-	-	9	3	-	-

* Reference film, only for release studies.
** Placebo films, only for disintegration tests.

2.4. Viscosity of the solutions

The viscosity of polymer solutions and formulations was measured with a Brookfield Viscometer DV2T (Middleboro, MA, USA), using a 52Z spindle, setting an endpoint of 2 min. The sample volume was 500 μL, and measurements were performed in triplicate at 25 °C. HPMC solutions were measured at a speed of 0.6 RPM, while the measuring speed was adjusted for chitosan and EC solutions due to their lower viscosities.

2.5. Film preparation

Films were prepared by solvent casting in a Petri dish placed on top of drawings of circles of desired diameter (outer diameter 2.1 cm and inner diameter 1.7 cm) (Fig. 1). The backing layer was prepared by depositing 0.80 g of the chitosan solution (2 or 3% w/w) in a circle with a diameter of 2.1 cm. For the EC reference, 0.3 g of the EC (8% w/w) solution was used. The layer was left to dry overnight at ambient temperature. On the following day, 0.50 g of the drug-containing HPMC layer (9% and 2.8% w/w) was deposited on top of it with a diameter of 1.7 cm. This layer was dried overnight at ambient conditions. During preliminary studies, the polymer concentration was carefully optimized with respect to the viscosity of the film solution in order to minimize the formulation spreading beyond the target diameters and/or shrinking during the drying process. Fig. 1 shows a visual representation of the film preparation process. The chitosan layer was made slightly larger because the film is intended for buccal application with the drug-containing HPMC-layer facing the mucosa, while chitosan's mucoadhesive properties ensure contact and prolonged residence on the mucosal surface.

2.6. Film characterization

2.6.1. Visual inspection

The films were visually inspected for transparency, surface smoothness, presence of bubbles, and any potential signs of drug crystallization or irregularities.

2.6.2. Uniformity of mass and thickness uniformity and outer diameter

The films (N = 10 for film formulations and N = 3 for references) were weighed, and the average weight and standard deviation (SD) were recorded. The film thickness was recorded using a micrometer screw (Cocraft 0–25 mm ± 0.04 mm, Clas Ohlson, Sweden) at five different points; in the center and four different spots at the outer edges of the HPMC-containing layer. Averages and SDs for the thickness of five spots per film were calculated. The dimensions of the film at two outer diameters (perpendicular to each other) were also recorded. An average diameter was taken for each film (N = 10), and the average diameter and SD were calculated for each formulation.

2.6.3. Wide-angle X-ray scattering (WAXS)

Wide-angle X-ray scattering (WAXS) experiments were performed to determine the solid-state of the drug in the film for selected formulations (BPA bilayer films with 3% chitosan, i.e., B5, B6, B7 and B8). Mat:Nordic (SAXSLAB, Denmark) instrument equipped with a Cu Kα radiation source was used. Measurements were performed at room temperature under vacuum conditions (3 mbar). Data were collected for 300 s within the q-range of 0.07–2.7 $Å^{-1}$. Q-calibration in WAXS mode was achieved using LaB_6 powder. All scattering profiles represent azimuthally averaged curves. The spot size was 5 mm. All films were produced and analyzed in duplicates. Visually appearing clear films were analyzed at a single spot, whereas hazy films were analyzed at both hazy and clear sites. Formulations with a higher drug loading (15–20 mg) than in the films in Table 1 were additionally prepared and tested to reveal the estimated drug loading limit for BPA-loaded bilayer films.

2.6.4. Fourier Transform Infrared Spectroscopy (FT-IR)

Single-layered HPMC films with 10 mg drug loading were tested with FT-IR (Nicolet i5, Thermo Fischer Scientific, MA, USA) to determine the potential interactions of drug-HPMC. References (raw materials), physical drug-HPMC mixtures, as well as placebo films were also tested. The spectra were recorded in the transmittance mode with a resolution of 4 cm^{-1} and 16 scans in the wavelength interval between 500 and

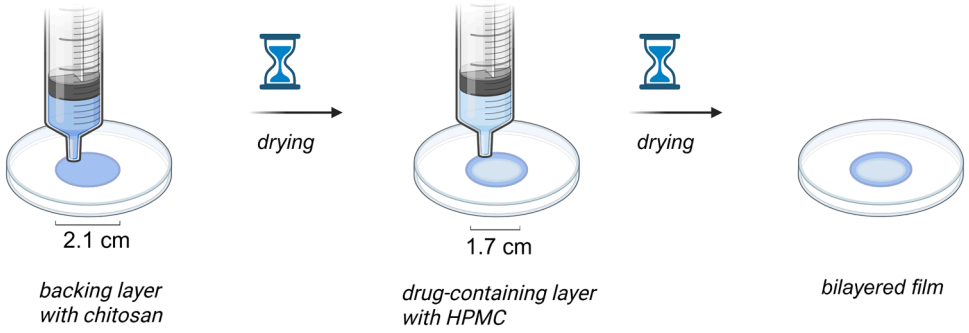

Fig. 1. Schematic representation of the film preparation process. The chitosan solution is deposited onto a Petri dish surface (circular shape with a diameter of 2.1 cm; blue color). The layer is left to dry overnight into a film, followed by depositing the second layer of the drug-HPMC solution with drug (diameter of 1.7 cm; light blue color) on top of it. The solution is left to dry overnight, forming a bilayer film. Figure was created with BioRender.

4000 cm^{-1}.

2.6.5. pH of the films

The pH of the films was recorded by adding 5 mL of milliQ water to the films in a small beaker and leaving them to swell for 5 min at room temperature (RT). Afterward, the film was removed, and the pH of the water was recorded using a pH meter (Five easy F20, Mettler Toledo Inc., Columbus, OH, USA). The experiment was performed in triplicate.

2.6.6. Swelling index

The swelling index of the bilayer films was determined by weighing a film (m_1) and placing it in a Petri dish containing 5 mL of PBS (pH 7.4) at 37 °C and allowing it to swell for 5 min. The excessive medium was gently wiped using tissue paper, and the hydrated films were weighed again (m_2). The swelling index was calculated according to Eq. (1). The experiments were performed in triplicate.

$$Swelling\ index = \frac{(m_2 - m_1)}{m_1} \quad (1)$$

2.6.7. Disintegration

To simulate agitation in the buccal cavity, disintegration tests were performed using a Petri-dish method. A film was placed in a lid-covered flask with 10 mL PBS. The flask was incubated at 37 °C and shaken at 60 rpm using a shaker incubator (Environmental Shaker-Incubator ES-20, Biosan, Latvia). The films were observed for loss of the coherent matrix (disintegration of HPMC layer), i.e. loss of the circular shape of the film. An additional observation was the complete loss of the matrix (i.e. disintegration of the chitosan film). The experiment was performed in triplicate for up to 60 min. In order to elucidate whether disintegration of the HPMC layer was a result of the film thickness or the Mw of the polymer, placebo films were tested (see Table 1) in both HPMC concentrations, i.e. both 2.8% and 9% for HPMC LM and HPMC HM.

2.6.8. Drug content

The drug content in BPA-containing formulations was quantified by adding 50 mL of PBS buffer to a flask containing a film. The flask was sonicated for 15 min and stirred with a magnetic stirrer for 75 min. The solution was filtered through a 0.20 μm cellulose acetate filter (VWR International, LLC, West Chester, PA, USA) to remove undissolved polymer and quantified by UV–VIS spectroscopy (SpectraMax 190, Molecular Devices, CA, USA) at 262 nm. The calibration curve provided $R^2 > 0.999$ (10–1000 μg/mL).

For quantification of the drug in TCA-containing formulations, 30 mL of 50% ethanol/water solution was added to a flask containing a film, as PBS was insufficient to fully dissolve the drug. The flask was sonicated for 25 min and then stirred at 60 rpm and 37 °C for another 35 min. The solutions were filtered through the same type of cellulose acetate filter as above and quantified by UV–VIS spectroscopy at 310 nm. The calibration curve provided $R^2 > 0.999$ (0.1–50 μg/mL). The drug quantification experiments were performed in triplicate.

2.6.9. Drug release

The release test was performed using side-by-side cells with an outer orifice of 2.6 cm and an inner orifice of 1.2 cm (PermeGear, PA, USA). A bilayer film piece was mounted between the two cells without any additional membrane, which was then attached together with the screws. 3.4 mL of 0.01 M PBS (pH 7.4) was added simultaneously to each side, and the solutions were stirred at the bottom of each cell using a magnetic stirrer. Samples of 100 μL were collected at predefined time points from both compartments (0.5, 1, 2, 3, 5, 7.5, 10, 15, 20, 30, 45 and 60 min) and diluted with PBS. The withdrawn amount was immediately replaced with PBS. The experiment was performed at 37 °C. Sink conditions were maintained in both compartments. The drug was quantified using UV–VIS spectroscopy with Multiplate UV reader (SpectraMax 190, Molecular Devices, CA, USA). The placebo reference films were also tested for a potential polymer-scattering effect. Additionally, films with 10 mg BPA drug loading (without a backing layer and with an EC backing layer) were tested as references. All experiments were performed in triplicate.

To assess whether dissolved polymer would influence the analytical results using a direct UV method, placebo films (P3 and P4) were tested in the same setup. Absorbance corresponding to the background of the placebo films (Supplementary material, Fig. S2) was therefore subtracted to only account for the drug for all formulations measured at 262 nm (BPA) and for HPMC HM formulations at 310 nm because of the interference with the absorption of the polymer with the drug at this wavelength (see Supplementary material, Fig. S3).

The shielding effect obtained from the chitosan backing layer was evaluated by comparing the cumulative release from the backing compartment to that from the drug-containing compartment during the simultaneous release experiment. At each time point, the shielding effect was calculated as:

$$Shielding\ effect = 1 - \frac{release_b}{release_d}$$

Where $release_b$ and $release_d$ refer to the cumulative amount of drug released from the backing side and the drug side, respectively. This parameter reflects the extent to which the backing layer limits drug diffusion through the backing side of the bilayer film and into the oral cavity.

2.6.10. Ex-vivo permeability studies

Franz cells (PermeGear, PA, USA) with a diameter of 11.28 mm and 8 mL acceptor volume were used to determine *ex vivo* permeability of two chosen film formulations (B5 and T3, i.e., bilayer HPMC LM films with 3% chitosan containing 5 mg BPA and TCA, respectively). The acceptor was filled with PBS until reaching the membrane height, and the 17 mm ready-to-use PermeaPad® biomimetic membrane (Phabioc GmbH, DE) was placed in between the compartments. 1 mL of PBS was added to the donor chamber, and the membrane was left to hydrate for 20 min. A film piece (N = 5), with a surface area corresponding to the effective diffusion area (1.00 cm^2), was cut and placed onto the membrane with the drug layer facing the membrane (theoretical average drug loading 3.6 mg/film and 4 mg/film for BPA and TCA, respectively). The acceptor chamber was stirred at the bottom at 500 rpm throughout the experiment. The experiments were performed at 37 °C for 5 hours, and 0.2 mL samples were collected at 30, 60, 90, 120, 180, 240 and 300 min. The withdrawn volume was replaced with PBS each time. Sink conditions were maintained in the acceptor chamber. The samples were diluted if necessary, and the drug was quantified using the same multiplate reader as above. Additionally, the drug references (dissolved in PBS) were tested in triplicate. The linear slope of the permeation curves (flux) was used to calculate the apparent permeability coefficient (P_{app}) of the formulation by normalizing it over the total theoretical drug content on the donor side.

2.6.11. Statistical analysis

The results are expressed as mean ± SD. A two-sided student *t*-test and ANOVA with Tukey post-hoc were performed where applicable. The difference between samples was considered significant when the p-value was lower than 0.05 (confidence interval = 95%).

3. Results and discussion

The chitosan chosen for this project is an ultrapure type of pharmaceutical grade called Chitopharm™, which is developed especially for drug delivery and wound dressings. It has high biocompatibility and induces minimal inflammatory response (Chitinor, n.d.). This chitosan should therefore be well suited for buccal drug delivery in patients with mucosal lesions and ulcers. Chitosan has been described as astringent

due to the positive charge density (Luck et al., 2015). Astringency might be an advantage with respect to contraction of vessels in the inflamed mucosa, which could potentially contribute to pain relief in combination with the selected drugs BPA and TCA that are known to induce dose-dependent vasoconstriction (Hoff et al., 1994). This is expected to provide local pain relief and reduce the systemic distribution of the drugs.

3.1. Viscosity of the wet formulations

The concentration of the chitosan solution was aimed to be high enough to provide a shielding effect of the backing layer, but low enough to minimize the amount of lactic acid needed to dissolve the polymer. To facilitate the easy deposition of the first layer onto the Petri dish, chitosan solutions with low viscosity were used. 2% and 3% w/w were deemed suitable concentrations to reach this balance. The chosen HPMC LM and HPMC HM concentrations for the drug-containing film formulations were based on concentrations giving viscosity of the polymer solutions. The aim was to choose concentrations that would yield high enough viscosities to easily cast the second HPMC-drug layer on top of the chitosan layer without it being spilled, and at the same time to have similar viscosities for both HPMC solutions regardless of Mw. A viscosity around 10 Pa × s seemed suitable. The viscosity experiments were performed at lower rotational speeds for HPMC solutions than those used for the chitosan and EC solutions. Table 2 shows the viscosities of the polymer solutions. The HPMC formulations exhibited viscosity ranging from 8.3 to 13.8 Pa × s, providing a suitable viscosity range for controlled deposition of the drug layer onto the backing layer. Increasing drug concentration from 10 to 20 mg/g resulted in a significant increase in viscosity, indicating potential drug-polymer interactions ($p < 0.05$) in all drug-polymer combinations, except for BPA-HPMC HM where the increase is non-significant ($p > 0.05$). This could suggest formation of weak bonds, such as hydrogen and hydrophobic interactions between drug(s) and polymers. After administration into the buccal cavity, the bilayer films undergo hydration, swell, and form a hydrogel. The viscosity of the chitosan hydrogel is expected to reduce the amount of drug release through the backing layer, and the hindering effect is expected to increase with increasing chitosan concentration.

3.2. QCM-D

Using AFM, homogeneity of the chitosan film after preparation and stabilization on a QCM-D sensor was confirmed (see Supplementary material, Fig. S1). The frequency and dissipation response for adsorption of HPMC LM and HPMC HM (Fig. 2) onto the chitosan surface showed that the frequency decreases with injection of both types of HPMC, indicating that the HPMC adsorbed onto the chitosan interface (Easley et al., 2022). The frequency increased by less than 15% of the maximum value but did not return to the level after rinsing with water, suggesting that the adsorption was irreversible. The increasing dissipation values after rinsing the surface with HPMC solution show that the adsorption resulted in the layer becoming viscoelastic (Easley et al., 2022). Based on the Johannsmann equation, the absorbed mass was calculated to be 18.7 ± 3.4 and 25.9 ± 2.2 mg/m^2 for HPMC LM and HPMC HM, respectively, without a significant difference between the two HPMC types. This is in the same order of magnitude as reported for HPMC 60 SH 4000 (Arumughan et al., 2026). They reported an effect of the substitution on the HPMC 4000 grades on the absorbed mass on the chitosan film. The HPMC grades in the current study, even though the HPMC HM is a HPMC 4000 grade, are less well-characterized; nevertheless, the absorbed mass seems to be in the same order of magnitude. This data suggests that chitosan and HPMC interact with each other, and that preparation of bilayer films could be expected to stick tightly together, even after drying.

Table 2
Viscosity of the polymer solutions, measured at 0.6 RPM. The values (N = 3) are presented as average ± SD.

Formulation	Viscosity (Pa × s)
9% HPMC LM, 10 mg/g BPA	10.2 ± 0.3
9% HPMC LM, 20 mg/g BPA	13.4 ± 0.4
9% HPMC LM, 10 mg/g TCA	8.5 ± 0.2
9% HPMC LM, 20 mg/g TCA	9.3 ± 0.2
2.8% HPMC HM, 10 mg/g BPA	11.4 ± 0.9
2.8% HPMC HM, 20 mg/g BPA	13.1 ± 0.0
2.8% HPMC HM, 10 mg/g TCA	11.1 ± 0.5
2.8% HPMC HM, 20 mg/g TCA	12.2 ± 0.1
2% chitosan CM in 1% LA	0.7 ± 0.0 *
3% chitosan CM in 1.5% LA	2.6 ± 0.1 **
8% ethyl cellulose in 96% EtOH	0.3 ± 0.0 ***

* 10 RPM.
** 3 RPM.
*** 200 RPM.

3.3. Films characterization

3.3.1. Visual inspection

The films were transparent (with a slightly yellow tone for HPMC LM), and no crystalline areas were visible at the chosen drug loadings of 5 mg and 10 mg. An example of a bilayer film piece is shown in the Supplementary material, Fig. S4. Some films contained smaller bubbles that occurred during the deposition of the solution onto the Petri dish. In some cases, the films would have a slightly concave shape in the middle. The irregularities, such as bubbles, can be attributed to the manual casting process, which makes achieving uniformity more challenging. The concave shape can be attributed to the skin formation during the drying and adhesion to the Petri dish surface, which restricts shrinkage at the edges and results in a thinner center. No delamination between the HPMC and chitosan layers was observed, supporting the findings from the QCM-D data. In contrast, the reference films with EC as a backing layer showed a tendency to delaminate, emphasizing the importance of selecting polymers with sufficiently strong polymer interactions to maintain interlayer adhesion for the preparation of bilayer films.

3.3.2. Solid state analysis

All bilayer film formulations B1-B8 and T1-T4 containing 5 mg or 10 mg of drugs (BPA or TCA, respectively), appeared clear, without visible crystals, whereas formulations tested at higher drug loadings (> 10 mg) showed white, crystalline-like areas. WAXS showed that the studied film formulations containing 5 and 10 mg BPA did not result in products with crystalline drug (see Fig. 3). Only 20 mg BPA HPMC LM and 15 mg BPA HPMC HM (i.e., higher drug loading than in B1-B8 formulations) were found to have a visually hazy appearance (see Supplementary material, Fig. S5). Films containing TCA were not included in the WAXS studies. As expected, the visually hazy films showed crystalline peaks in WAXS. These films contained both clear and hazy areas, and the hazy areas could be related to the crystalline drug, as shown in WAXS data. These results provide the foundation for selecting the formulations containing 5 and 10 mg of BPA dispersed in an amorphous state within the polymer.

FT-IR spectra for BPA/HPMC formulations showed characteristic shifts for various BPA functional groups (Martins et al., 2017; Souza de Freitas Domingues et al., 2022) (Fig. 4a and Supplementary material, Fig. S6) and revealed structural changes upon film formation. The IR bands for BPA observed at 1654 and 1687 cm^{-1} correspond to the C = O stretching of the amide group. In the films, they merge into a single broader peak at 1683 cm^{-1}, indicating hydrogen bonding interactions between the BPA and the -OH groups in HPMC. The BPA band at 1563 cm^{-1} corresponds to N—H bending of the amide, which shifts to 1540 cm^{-1} in the film, indicating interactions between BPA and HPMC, specifically N—H hydrogen bonding with the hydroxyl group in HPMC. The band at 3506 cm^{-1} corresponds to the N—H bond stretching. Both BPA-HPMC films showed a broadened and shifted peak (3441 cm^{-1})

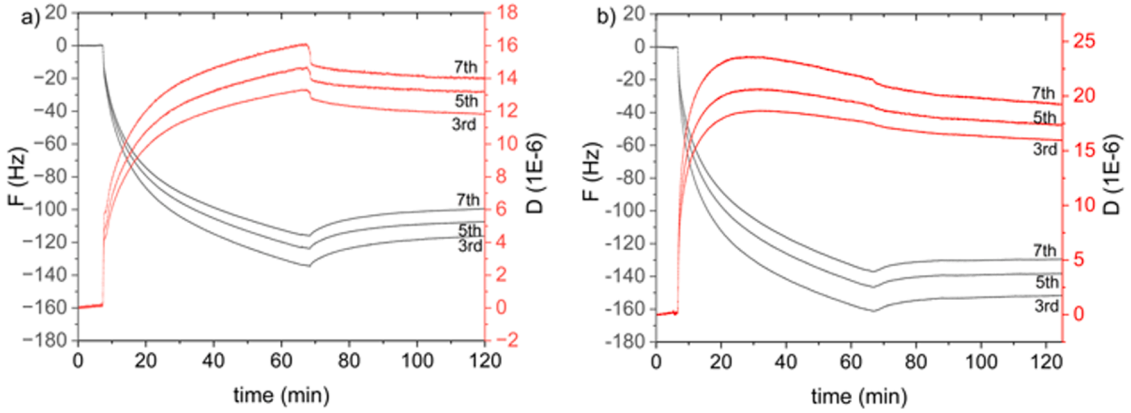

Fig. 2. Representative frequency and dissipation response onto a chitosan surface of a) HPMC LM and b) HPMC HM.

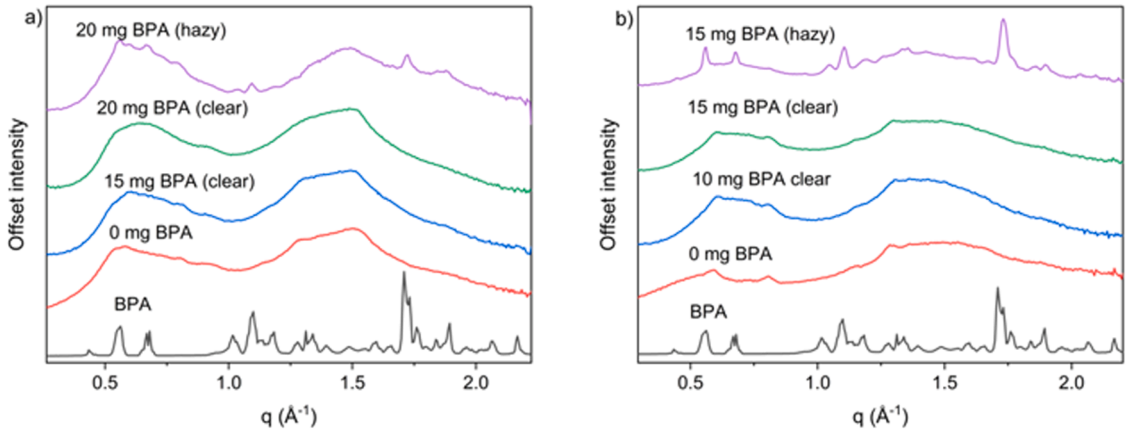

Fig. 3. WAXS scattering curves of chosen samples containing HPMC and various BPA drug loadings. Fig. 3a) represents films with HPMC LM. The sample with 20 mg BPA LM (hazy) contains crystalline BPA, while lower drug loadings contain BPA in the amorphous state. Fig. 3b) represent films with HPMC HM. The sample with 15 mg BPA contains crystalline BPA, while lower drug loadings contain BPA in amorphous state.

compared to the raw material of HPMC LM or HPMC HM polymers (3456 cm^{-1} and 3451 cm^{-1}, respectively), additionally indicating drug-polymer interactions between the N—H (BPA) and O—H (HPMC LM).

The FT-IR spectra for TCA/HPMC samples (Fig. 4b) showed a band at 1688 cm^{-1} for TCA, corresponding to the C = O stretching of the ester (Dennis et al., 2004). This band broadens and shifts to around 1700 cm^{-1} for the TCA-HPMC LM and TCA-HPMC HM films, respectively, indicating hydrogen bonding with the hydroxyl group of HPMC. The band at 1598 cm^{-1} for TCA corresponds to N—H bending or aromatic ring vibrations, shifting to 1604 cm^{-1} in both drug-polymer films, indicating weak hydrogen bonding or dipole-dipole interactions with the hydroxyl groups of the polymer. The TCA spectra show a band at 3373 cm^{-1}, indicating N—H stretching. This band broadened and shifted to 3441 cm^{-1} in the film formulations, indicating interactions with the hydroxyl groups in HPMC. These results showed that both drugs interacted with HPMC.

Overall, the FT-IR results indicate the formation of both hydrogen bonds, dipole-dipole interactions and hydrophobic interactions between the drugs and HPMC in the dried films, which could support the observed increase in viscosity for drug-HPMC solutions discussed above.

3.3.3. *Uniformity of mass, thickness and geometry*

The films were prepared based on weight. Film from formulations with HPMC HM weighed 45.7–66.3 mg and formulations with HPMC LM weighed 78.8–103.9 mg (see Table 3). The formulations with HPMC LM had a higher weight due to the higher polymer concentration in the cast solution (i.e. higher dry content in the film). Between zero and three out of 10 films weighed had a weight deviating from an average of up to 5% (depending on the formulation), and none deviated more than 10% for all formulations. These results indicate acceptable mass unitformity witin the batch for single-dose preparations, although the pH.Eur. 2.9.5 (unit mass less than 250 mg) requirement of 20 units was not applied (Council of Europe, 2014).

Although the films were deposited by weight, working with high-viscosity formulations can result in a larger variability, which can further increase when depositing two layers on top of each other. This can also result in differences in film thickness at various film spots, despite lower variability when averaging five values per film. The average film thickness for each formulation is shown in Fig. 5a. Films prepared with HPMC LM were significantly thicker than films with HPMC HM ($p < 0.05$). No meaningful differences were determined between formulations within each group, suggesting that the thickness was directed by the HPMC type, or in other words, the polymer concentration. The average outer diameter ranged from 1.9 to 2.1 mm across all formulations (Table 3), indicating that some formulations deviated slightly from the target diameter of 2.1 mm. Adjusting the size of the films could be done for patients with bigger ulcers, as well as using several films at the same time at different places in the buccal cavity.

The pH of the formulations ranged from 4.23 to 4.56 (Table 3), without any clear trends between the formulations. Excessively acidic (pH < 4) or alkaline (pH > 8) formulations are known to cause irritation when applied to the mucosa (Preis et al., 2013). At the same time, pH below the critical pH (around 5.5) increases the tooth decay process

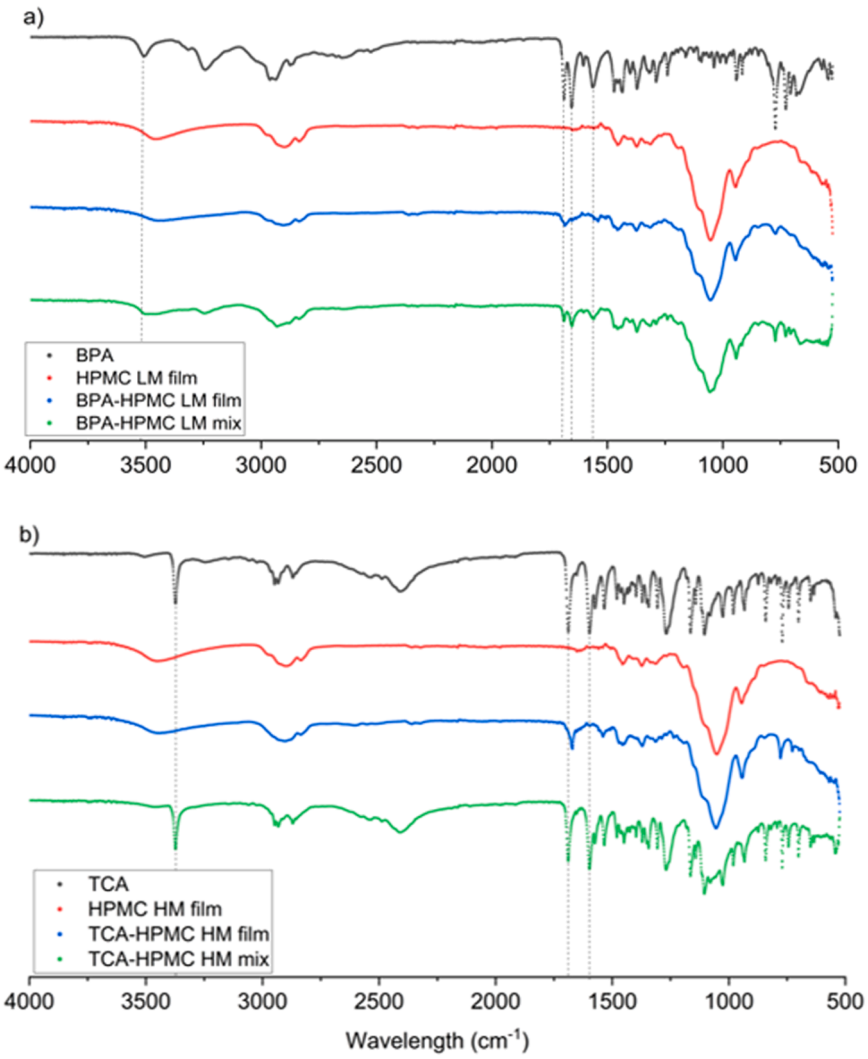

Fig. 4. FT-IR spectra of a) BPA raw material, HPMC LM film, BPA-HPMC LM film and physical mixture of BPA and HPMC LM and b) TCA raw material, HPMC LM film, TCA-HPMC LM film and physical mixture of TCA and HPMC LM.

(Dawes, 2003). The tested formulations, even though on the weak acidic side, show pH values above the reported pH range of juices (pH 2.6–4.1) and apple sauces (pH 3.3–3.9) and overlapping with yoghurts (pH 3.7–4.5) (Eckert et al., 2025), all food and drinks that might be accepted in oral mucositis patients. The tested formulations have a pH lower than that of the buccal environment, but are beneficial for chitosan protonation and mucoadhesion (Alves et al., 2020). Additionally, the therapy duration should ideally not be longer than some weeks. Therefore, relieving the pain and enabling the patients to eat, swallow, and speak and avoid potential malnutrition and pain will increase the quality of life and potentially avoid or reduce the need for parenteral opioids.

The obtained drug content of the formulations is shown in Table 3. The drug content for BPA was, on average, corresponding to the theoretical loading. It varied for formulations with 5 mg BPA from 4.7 to 5.7 mg, and for formulations with 10 mg BPA from 9.3 to 11.1 mg. The deviation for TCA formulations was higher, with the measured drug content lower than the theoretical loading value, potentially due to interactions with the film matrix or drug losses during the experiment.

The films containing HPMC and chitosan are expected to be mucoadhesive, as both polymers have been shown earlier to be mucoadhesive (Tzanova et al., 2021; Korelc et al., 2023). Mucoadhesion of the formulations was therefore not tested in this work. As chitosan forms a backing layer, there is a possibility for its adhesion to adjacent mucosal surfaces (e.g., between the gum and the cheek) upon application. However, this behavior is difficult to predict and would require additional evaluation using relevant biological models. Nevertheless, natural movements in the oral cavity (i.e., speaking, swallowing, saliva flow) were expected to minimize unintended adhesion. The films should provide a pleasant mouthfeel as they swell when in contact with saliva, forming a smooth gel surface in the mouth, and in addition, covering a painful sore area, protecting it from external conditions. The chitosan layer is further expected to contribute to antimicrobial and wound-healing effects (J. Su et al., 2025); however, this was beyond the scope of the current work and has not been studied.

3.3.4. *Swelling and disintegration*

The swelling index is a measure of the water-uptake capability of the film. Table 3 shows the swelling index for the films after 5 min of hydration with PBS pH 7.4. The swelling of the film is crucial for mucoadhesion, but can also affect disintegration (Preis et al., 2013). On the other hand, the swelling should not be excessive, as it can cause discomfort in the buccal cavity. The swelling index ranged from 2.1 to 9.4, indicating that the water molecules easily penetrate the polymer matrices. The results are in line with literature values for swelling index values of various chitosan-based films (Paczkowska-Walendowska et al., 2025). As expected, the swelling index was significantly higher for HPMC HM films in direct comparison with HPMC LM films; B5/B7, T1/T3 and T2/T4 ($p < 0.05$). For the buccal application, it is important

Table 3
Basic properties of the bilayered films (N = 10). The results are recorded as average ± SD.

Formulation	Mass (mg)	Outer diameter (cm)	pH *	Drug content (mg) *	Swelling index *
B1	82.5 ± 3.7	2.0 ± 0.1	4.30 ± 0.08	5.2 ± 0.3	5.5 ± 0.3
B2	86.8 ± 4.5	2.0 ± 0.0	4.29 ± 0.02	10.2 ± 0.5	3.2 ± 1.0
B3	46.1 ± 0.4	1.9 ± 0.1	4.29 ± 0.04	5.2 ± 0.1	8.2 ± 1.2
B4	51.5 ± 0.8	2.0 ± 0.0	4.34 ± 0.03	9.9 ± 0.5	6.3 ± 1.5
B5	94.4 ± 2.9	2.0 ± 0.1	4.33 ± 0.11	5.2 ± 0.5	2.7 ± 0.2
B6	100.6 ± 3.3	2.1 ± 0.0	4.43 ± 0.05	10.6 ± 0.5	5.3 ± 0.7
B7	58.8 ± 1.1	2.0 ± 0.1	4.41 ± 0.11	5.0 ± 0.1	4.8 ± 0.4
B8	65.0 ± 1.3	2.0 ± 0.0	4.45 ± 0.11	9.8 ± 0.5	6.3 ± 0.4
T1	91.6 ± 1.0	2.1 ± 0.0	4.35 ± 0.04	4.0 ± 0.4	2.7 ± 0.3
T2	100.3 ± 2.2	2.0 ± 0.0	4.40 ± 0.11	7.6 ± 0.6	4.9 ± 0.6
T3	59.5 ± 1.0	2.0 ± 0.1	4.40 ± 0.03	4.7 ± 0.3	2.3 ± 0.2
T4	65.0 ± 1.0	2.1 ± 0.0	4.29 ± 0.06	8.9 ± 0.5	5.0 ± 0.4

* N = 3.

that the swelling of a bilayer film is homogeneous to ensure successful mucoadhesion to the buccal mucosa. A figure of the swollen film piece is shown in Supplementary material, Fig. S7 to show that both layers contributed to swelling, resulting in a uniformly swollen film and that the brim remains attached to the surface after swelling. The swelling of the films was deemed suitable for the formulations without the excessive increase in size when they hydrate.

During the 60-min disintegration test, the HPMC layer disintegrated, and the film lost its shape. The chitosan matrix remained visible throughout the experiment, as the chitosan films are not expected to disintegrate in the PBS (Korelc et al., 2023). The disintegration of the HPMC layers differentiated the formulations from each other (see Fig. 5b). The main film lost its shape after approximately 40 min for HPMC LM formulations and after only approximately 20 min for HPMC HM formulations. Pictures illustrating the disintegration behavior are shown in the Supplementary material, Fig. S8. HPMC HM would generally be expected to slow down water uptake and disintegration due to higher molecular weight (Reynolds et al., 1998). However, due to the difference in the polymer concentration of HPMC LM and HPMC HM used in the films, the thinner HPMC HM films absorbed more media and disintegrated faster ($p < 0.05$). This was elucidated in a separate test with the disintegration of placebo films (P1-P4) together with their measured thicknesses (N = 3) (Fig. 5). The ANOVA showed that the film disintegration time was not dependent on the formulation within the same HPMC type ($p > 0.05$). These results confirmed that film thickness, not the HPMC Mw, is the main factor contributing to the film's disintegration rate.

It should be kept in mind that the disintegration test performed here is not biorelevant. When the bilayer film is adhered to the mucosal membrane, the chitosan layer will serve as an insulating barrier and the disintegration of the HPMC layer is expected to be slower. Nevertheless, the information gained using this method is relevant because it ranks the formulations with respect to the solubility of the drug-containing HPMC layer, which would be linked to the drug release rate. This contributes to understanding the drug release behavior.

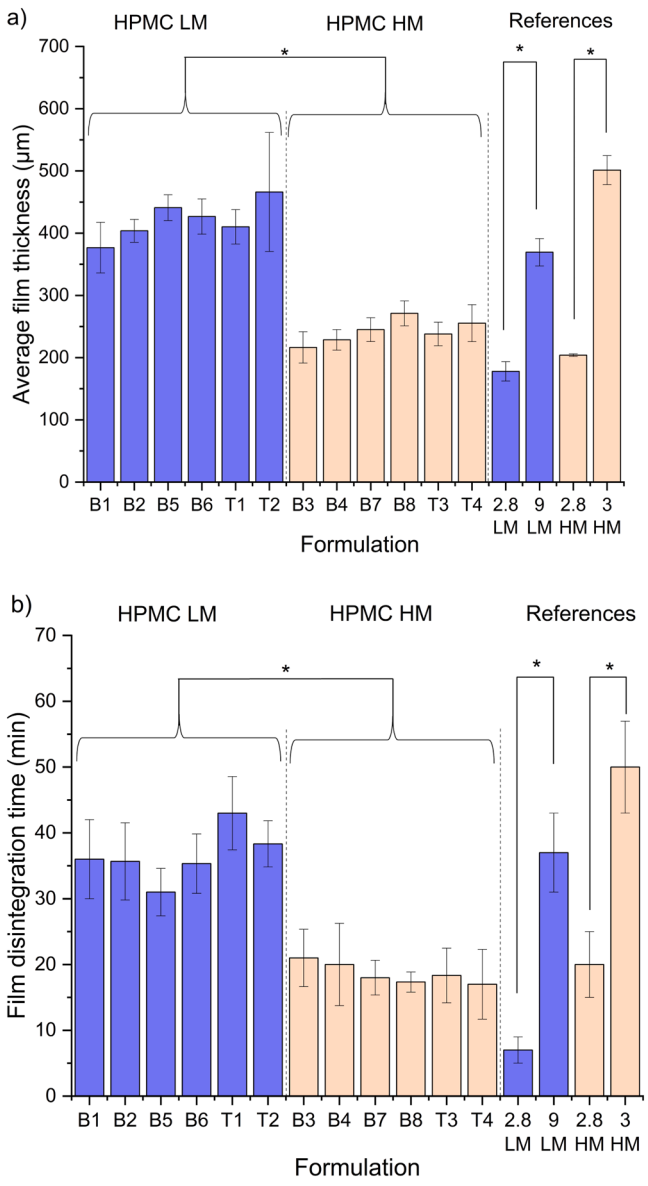

Fig. 5. a) Average film thickness (N = 10 for film formulations and N = 3 for references) and b) average disintegration time of formulations (N = 3) (average ± SD). Statistically significant differences in film thickness and disintegration time between HPMC LM and HPMC HM films are marked with an asterisk ($p < 0.05$).

3.3.5. *Release studies*

Using the side-by-side cell, the release was monitored simultaneously in both chambers and expressed as drug released from the drug-containing layer and the backing layer of the bilayer film. The release profiles for the selected HPMC LM formulations are shown in Fig. 6, and for the remaining formulations in the Supplementary material, Fig. S9. Release from the drug-containing layer was similar among formulations with the same drug, drug load, and HPMC type (solid lines in Fig. 6a: B1, B5, and Fig. 6b: B2, B6). Formulations with 2% chitosan (B1-B4) showed that the backing layer did not hinder the drug release to any larger extent compared to the drug side. Increasing the chitosan concentration to 3% (B5-B8, T1-T4) produced a greater difference between release from the two sides, consistent with a shielding effect of the backing layer, particularly for HPMC LM (Fig. 6a: B1 vs B5 and Fig. 6b: B2 vs B6). In formulations containing 3% chitosan and HPMC LM, the release rate through the chitosan layer was reduced throughout the experiment, resulting in a significantly greater amount of drug released through the

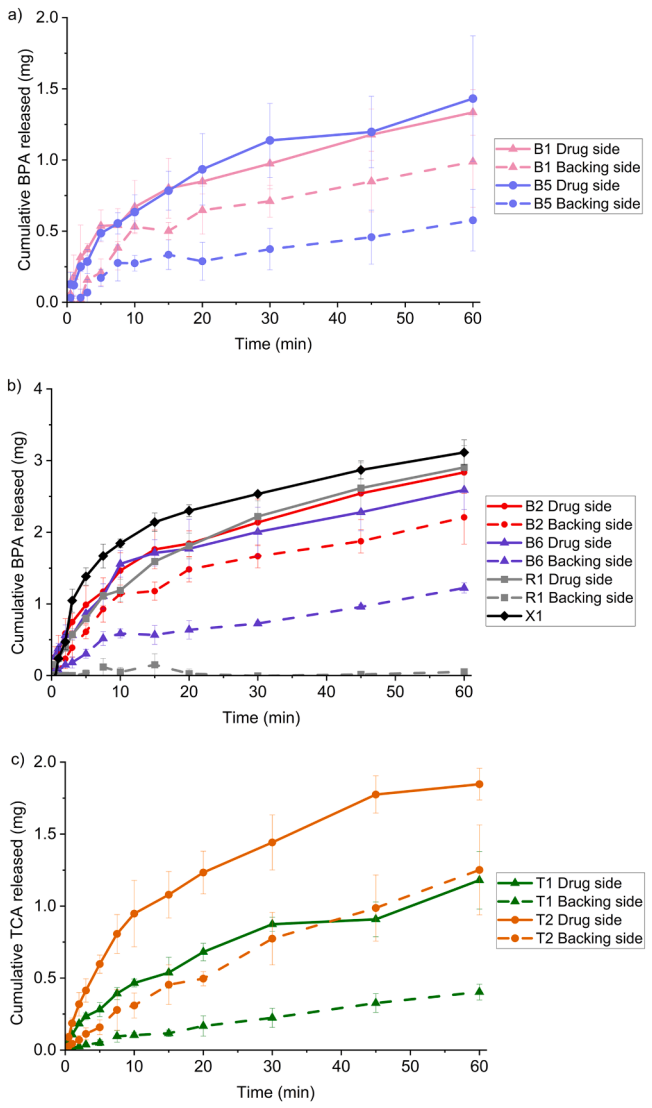

Fig. 6. Drug release curves containing release from the drug side and the backing side (average ± SD, N = 3) for a) 5 mg BPA-HPMC LM films with 2% chitosan (B1) and 3% chitosan (B5), b) 10 mg BPA-HPMC LM films with 2% chitosan (B2), with 3% chitosan (B6), with EC as backing layer (R1) and a single-layer HPMC LM film with no backing layer (X1), c) TCA-HPMC LM films with 3% chitosan and 5 mg (T1) and 10 mg (T2) TCA.

drug layer than through the backing layer. Drug release was followed for 1 h. At the end of the experiment, the HPMC LM films containing 3% chitosan remained swollen, indicating that the backing layer had not disintegrated (see Supplementary material, Fig. S10). A shielding effect of the chitosan backing layer was observed for both drugs. In contrast, the amount of drug released through the EC backing layer (reference), was negligible (Fig. 6b), as expected. EC is a water-insoluble, essentially impermeable biocompatible polymer suitable as a film former for flexible films (X. Su et al., 2020), but it lacks mucoadhesive properties and is likely to protect the wounded area less effectively than swollen chitosan gel.

Formulations with HPMC HM were less effective in hindering drug release through the backing layer. They provided some initial shielding at the initial stage of the experiment (within the first 10 min), after which the release rate became similar from both compartments (see Supplementary material, Fig. S9). The lack of shielding can be attributed to the visible disintegration of HPMC HM films after 7–10 min in aqueous medium, leading to disruption of the chitosan backing layer, and free diffusion of drug between the two compartments. Polymer fragments were observed in the media, and the HPMC HM films were clearly disintegrated at the end of the experiment. Release data for B3 and B7 are not included because the BPA quantification was unreliable due to high background scattering relative to the drug signal. These formulations also disintegrated rapidly and showed little potential for achieving unidirectional release.

The disintegration behavior observed in the release experiments is not directly comparable to that in the dedicated disintegration test, owing to differences in the experimental setup. In the side-by-side cell, the film is fixed between two compartments, and the magnetic stirrer at the bottom generates different flow patterns in the compartments. In the disintegration test, the films move freely in PBS, exposed to slower and more uniform flow. Nevertheless, both methods are purely in vitro and not biomimetic. In vivo, both disintegration and drug release are expected to be slower due to lower liquid volumes and the insulating effect of the chitosan backing layer.

It should be noted that due to the orifice diameter of the side-by-side cell (1.2 cm), the drug-containing layer (diameter 1.7 cm) was not completely exposed to the media. The estimated area available for release corresponded to the 1.3 cm diameter (i.e., approximately 58% of the drug-containing area). Adjusted for the area available for drug release, formulations with HPMC LM released in total to 65–87% of BPA and 53–54% of TCA during the one-hour experiment, while films with HPMC HM released 45–51% of BPA and 54–65% of TCA. It is worth noting that the non-exposed area can become partially hydrated, and therefore part of the drug is expected to diffuse from the non-exposed areas to the exposed areas. This variable was outside the scope of the study and was not further studied.

Even though disintegration and drug release were assessed using in vitro methods that do not fully mimic in vivo conditions, the data allow meaningful ranking of the formulations with respect to unidirectional release. In particular, the effectiveness of the backing layer in limiting drug release into the oral cavity. The shielding performance is summarized in Fig. 7. Formulations containing 3% chitosan and HPMC LM were estimated to hinder 32–66% of drug release through the backing layer within 1 h. As expected, the highest shielding was observed for EC reference formulations. Among the bilayer films with 3% chitosan as the backing layer, the strongest shielding was obtained for HPMC LM films with 5 and 10 mg BPA (B5 and B6) and 5 mg TCA (T1).

Films containing 3% chitosan and HPMC LM provided significantly greater shielding than those with 2% chitosan at 10 min ($p < 0.05$). After 30 minutes, this trend was still observed ($p < 0.05$) for all the formulations except T1, which lost more shielding than the rest of the films with 3% chitosan. After 60 min, the average shielding effect remained higher for formulations with 3% chitosan compared to 2% chitosan, but without statistical significance, likely due to swelling and partial disintegration of the film in the setup, which weakened the chitosan backing layer. In contrast, films containing HPMC HM showed no significant shielding beyond the initial minutes of the release experiment, irrespective of the chitosan concentration ($p > 0.05$). A shielding effect of about 60–70% after 1 h was considered acceptable. The fact that the chitosan is not an impermeable backing layer like EC, and therefore allows some drug to diffuse into the oral cavity, was not considered as problematic, as this may help numb additional painful areas. Although this implies less precise control of the pharmacokinetics, the fraction of the dose ultimately swallowed is expected to be small with minimal systemic absorption, while potentially contributing to local numbing of the esophageal lining.

Based on the extent of drug released from bilayer films, it is useful to compare the results to the doses used for the treatment of oral mucositis, studied in the literature. A study by *Mogensen* et al. investigated the use of a 25 mg bupivacaine lozenge for an anesthetic effect, which induced long-lasting pain relief without side effects over at least a 3-hour period in patients with oral mucositis after having dissolved (Mogensen et al., 2016). An in situ-forming gel containing 5–10 mg/mL bupivacaine γ-linoleate was developed by Li et al., and was deemed suitable to

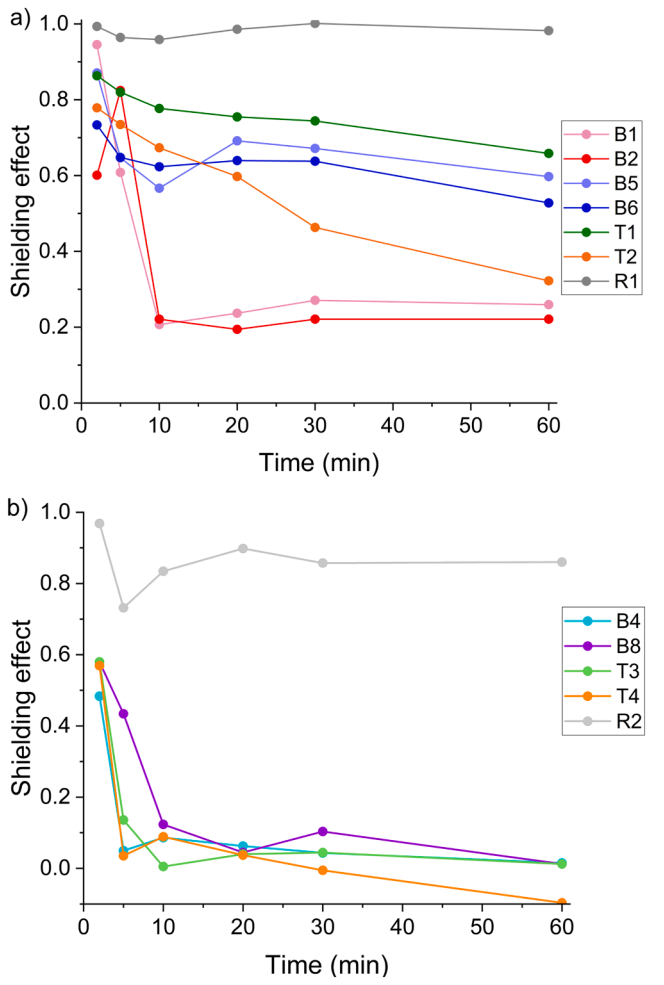

Fig. 7. Visual representation of the average shielding effect (N = 3) of the backing side at different time points for HPMC LM (top) and HPMC HM (bottom). Backing layers consisting of 2% chitosan (B1-B4), 3% chitosan for BPA (B5-B8), 3% chitosan for TCA (T1-T4), and EC for R1 and R2.

provide oral anesthesia (Li et al., 2020). In another study, the authors developed a 1.5% tetracaine HCl gel to be applied on the oral mucosa by a mouthwash, which reduced pain without side effects (Alterio et al., 2006). The most suitable formulations in this work appeared to be the bilayer films with 10 mg BPA or TCA. Hence, the drug loading in this work was lower than in the literature; however, mucoadhesive films are expected to provide a longer residence time and a more localized effect due to the placement directly on the painful area, potentially reducing the amount of the anesthetic required for administration. The duration of the drug release and pain relief is expected to be longer in vivo than estimated using the described in vitro methods in the current study.

3.3.6. *Permeability studies*

The apparent permeability coefficient (P_{app}) of the tested formulations is shown in Table 4 and the permeation curves for the tested formulations can be found in Supplementary material, Fig. S11. The formulations' permeability values were comparable to those for the reference (drug in PBS solution), and the obtained P_{app} for bupivacaine is in line with findings from the literature at the same temperature (37 °C) (Kulkarni et al., 2011). Both drugs belong to the BCS class I. TCA was found to have a significantly higher permeability than BPA, likely due to its lower molecular weight (300.8 g/mol versus 342.9 g/mol) and differences in logP (3.4 and 3.5 for BPA and TCA, respectively) (*DrugBank*, n.d.; *Sigma-Aldrich*, n.d.; Wiedmer and Sohn, 2024). Additionally, TCA has also been shown to interact with lipid membranes, resulting in membrane deformation and disruption (Hu et al., 2020). The data suggest that drug release, rather than permeability, is likely to be the rate-limiting factor in drug permeation across the membrane. This indicates that, upon application to the buccal mucosa, the released drug may permeate the epithelial tissues and potentially reach the systemic circulation. It should be noted that the PermePad® is a biomimetic membrane composed of a dry lipid layer sandwiched between two cellulose-hydrate membranes, resembling the cell membrane structure and is designed to study passive diffusion of drugs through a monolayer membrane, mostly investigated for intestinal permeability (di Cagno et al., 2015; Jacobsen et al., 2020). The absorption throughout the buccal mucosa will likely differ, as it is a more complex barrier with an epithelium consisting of multiple layers in addition to the mucus lining. Depending on the location in the oral cavity, the thickness and keratinocyte content of the mucosa vary, and so does the distance to the blood flow. Most drug transport across the oral epithelium occurs via passive diffusion via the transcellular and paracellular pathway (Patel et al., 2011). However, it has been studied for buccal absorption in the literature and compared to the TR146 cell model as well as buccal tissue models for certain drugs (Bibi et al., 2016; Kabedev et al., 2025). To summarize, it cannot be concluded, based on these experiments, whether the bilayer films will actually lead to systemic absorption of the drugs or not; however, the drug will be released in proximity to the oral mucosa where the lesions are and should be available to interact with local nerve cells and pain receptors.

Table 4
P_{app} of the tested formulations (average ± SD, N = 3–5).

Drug	Film P_{app} (10^{-5} cm/s)	Reference P_{app} (10^{-5} cm/s)
TCA	3.2 ± 0.2	3.4 ± 0.2
BPA	1.7 ± 0.2	1.6 ± 0.2

4. Conclusions

In this study, chitosan was evaluated as a backing layer in bilayer buccal films containing the local anesthetics bupivacaine and tetracaine for local drug delivery and pain management in oral mucositis. Chitosan was selected for its mucoadhesive and swelling properties, as well as its proposed wound-healing and antimicrobial effects, with the aim of covering painful lesions and improving mouthfeel. Depositing a drug-containing HPMC layer on top of the chitosan layer yielded bilayer films without visible delamination. The films enabled incorporation of up to 10 mg BPA per circular-shaped films (1.7 cm in diameter) without compromising the amorphous state of the drug. A chitosan concentration of 3% was identified as suitable for functioning as a backing layer that hinders drug release into the oral cavity. The shielding effect was more pronounced in formulations containing HPMC LM than HPMC HM, which is attributed to the higher HPMC LM concentration and the resulting greater film thickness, leading to slower disintegration and a prolonged shielding effect over 1 h. A shielding effect of 60–70% was considered appropriate. Partial drug release through the chitosan layer into the oral cavity was not regarded as detrimental, and may even be advantageous by extending the numbing effect to adjacent painful areas. Overall, this study provides insights into the design and in vitro performance of chitosan-backed bilayer buccal films and supports their potential as a promising platform for local pain management in oral mucositis.

CRediT authorship contribution statement

Karin Korelc: Writing – original draft, Visualization, Methodology, Investigation, Formal analysis, Data curation, Conceptualization. **Vishnu Arumughan:** Writing – review & editing, Methodology. **Åke Henrik-Klemens:** Writing – review & editing, Methodology, Investigation, Data curation. **Anette Larsson:** Writing – review & editing,

Supervision, Project administration, Methodology, Investigation, Data curation. **Ingunn Tho:** Writing – review & editing, Supervision, Resources, Project administration, Methodology, Funding acquisition, Conceptualization.

Declaration of competing interest

The authors declare that they have no known competing financial interests or personal relationships that could have appeared to influence the work reported in this paper.

Acknowledgements

This project was carried out as part of Nordic POP (Patient Oriented Products), a Nordic University Hub funded by NordForsk (project number 85352). We would like to express gratitude to Katerina Nezvalova-Henriksen and Bjarke Strøm Larsen for their valuable discussions. Åke Henrik-Klemens was supported by the "FibRe—a Competence centre for Design for Circularity: Lignocellulose-based Thermoplastics", partly funded by the Swedish Innovation Agency VINNOVA (Grant No. 2019–00047). The authors would like to acknowledge the generous gift of chitosan from Chitinor, Norway.

Supplementary materials

Supplementary material associated with this article can be found, in the online version, at doi:10.1016/j.ejps.2026.107530.

Data availability

Data will be made available on request.

References

Alterio, D., Jereczek-Fossa, B.A., Zuccotti, G.F., Leon, M.E., Omodeo Sale, E., Pasetti, M., Modena, T., Perugini, P., Mariani, L., Orecchia, R., 2006. Tetracaine oral gel in patients treated with radiotherapy for head-and-neck cancer: final results of a phase II study. Int. J. Radiat. Oncol. Biol. Phys. 64 (2), 392–395. https://doi.org/10.1016/j.ijrobp.2005.07.301.

Alves, T.F.R., Rios, A.C., Pontes, K., da, S., Portella, D.L., Aranha, N., Severino, P., Souto, E.B., Gonsalves, J.K.M., Nunes, R.D.S., Chaud, M.V., 2020. Bilayer Mucoadhesive buccal film for mucosal ulcers treatment: development, characterization, and single study case. Pharmaceutics 12 (7), 657. https://doi.org/10.3390/pharmaceutics12070657.

Arumughan, V., Korelc, K., Tho, I., Larsson, A., 2026. The influence of substituents of cellulose ethers on their interaction with chitosan surfaces. Colloid. Interface Sci. Commun. 70, 100867. https://doi.org/10.1016/j.colcom.2025.100867.

Bibi, H.A., Holm, R., Bauer-Brandl, A., 2016. Use of Permeapad® for prediction of buccal absorption: a comparison to in vitro, ex vivo and in vivo method. Eur. J. Pharm. Sci. 93, 399–404. https://doi.org/10.1016/j.ejps.2016.08.041.

Cheng, K.K.F., Molassiotis, A., Chang, A.M., Wai, W.C., Cheung, S.S., 2001. Evaluation of an oral care protocol intervention in the prevention of chemotherapy-induced oral mucositis in paediatric cancer patients. Eur. J. Cancer 37 (16), 2056–2063. https://doi.org/10.1016/S0959-8049(01)00098-3.

Chitinor. (n.d.). *Chitopharm*. Retrieved March 11, 2026, from https://chitinor.com/chitopharm/.

Council of Europe, 2014. European Pharmacopoeia, 9th ed. Council of Europe.

Dawes, C., 2003. What is the critical pH and why does a tooth dissolve in acid? J. Can. Dent. Assoc. 69 (11), 722–724.

Dennis, A.C., Mcgarvey, J.J., Woolfson, A.D., Mccafferty, D.F., Moss, G.P., 2004. A Raman spectroscopic investigation of bioadhesive tetracaine local anaesthetic formulations. Int. J. Pharm. 279 (1–2), 43–50. https://doi.org/10.1016/j.ijpharm.2004.04.012.

di Cagno, M., Bibi, H.A., Bauer-brandl, A., 2015. New biomimetic barrier Permeapad ™ for efficient investigation of passive permeability of drugs. Eur. J. Pharm. Sci. 73, 29–34. https://doi.org/10.1016/j.ejps.2015.03.019.

DrugBank. (n.d.). Tetracaine hydrochloride. Retrieved February 6, 2026, from https://go.drugbank.com/salts/DBSALT001125.

Easley, A.D., Ma, T., Eneh, C.I., Yun, J., Thakur, R.M., Lutkenhaus, J.L., 2022. A practical guide to quartz crystal microbalance with dissipation monitoring of thin polymer films. J. Polym. Sci. 60 (7), 1090–1107. https://doi.org/10.1002/pol.20210324.

Eckert, C., Stillhart, C., Wagner, L., Scheubel, E., Prevot, I., Lindenberg, M., Klein, S., 2025. Towards the development of a standard toolbox for compatibility testing of pediatric drug products with common dosing vehicles – fruit juice, apple sauce, yogurt, and pudding. Eur. J. Pharm. Biopharm. 217, 114868. https://doi.org/10.1016/j.ejpb.2025.114868.

Fahs, A., Brogly, M., Bistac, S., Schmitt, M., 2010. Hydroxypropyl methylcellulose (HPMC) formulated films: relevance to adhesion and friction surface properties. Carbohydr. Polym. 80 (1), 105–114. https://doi.org/10.1016/j.carbpol.2009.10.071.

Ghadermazi, R., Hamdipour, S., Sadeghi, K., Ghadermazi, R., Asl, A.K., 2019. Effect of various additives on the properties of the films and coatings derived from hydroxypropyl methylcellulose — A review. Food Sci. Nutr. 7 (11), 3363–3377. https://doi.org/10.1002/fsn3.1206.

Hoff, B., Fletcher, S.J., Rickford, W.J., Matjasko, M.J., 1994. Spinal anesthesia using a 1: 1 mixture ofBupivacaine and tetracaine for peripheral vascular surgery. J. Clin. Anesth. 6 (1), 18–22. https://doi.org/10.1136/rapm-00115550-198813011-00011.

Hu, S., Zhao, T., Li, H., Cheng, D., Sun, Z., 2020. Effect of tetracaine on dynamic reorganization of lipid membranes. Biochim. Biophys. Acta (BBA) - Biomembr. 1862 (9), 183351. https://doi.org/10.1016/j.bbamem.2020.183351.

Jacobsen, A.-C., Nielsen, S., Brandl, M., Bauer-Brandl, A., 2020. Drug permeability profiling using the novel Permeapad® 96-well plate. Pharm. Res. 37 (6), 93. https://doi.org/10.1007/s11095-020-02807-x.

Johannsmann, D., 2008. Viscoelastic, mechanical, and dielectric measurements on complex samples with the quartz crystal microbalance. Phys. Chem. Chem. Phys. 10 (31), 4516–4534. https://doi.org/10.1039/b803960g.

Kabedev, A., Tønning, M.H., Teleki, A., Bauer-Brandl, A., Jacobsen, A.C., 2025. Understanding the transport of drugs across biomimetic barriers of various phospholipid compositions using a combined experimental and computational approach. Colloids Surf. B: Biointerfaces 253, 114706. https://doi.org/10.1016/j.colsurfb.2025.114706.

Kaewjiaranai, T., Srisatjaluk, R.L., Sakdajeyont, W., Pairuchvej, V., Wongsirichat, N., 2018. The efficiency of topical anesthetics as antimicrobial agents: a review of use in dentistry. J. Dent. Anesth. Pain. Med. 18 (4), 223–233. https://doi.org/10.17245/jdapm.2018.18.4.223.

Kamel, S., Ali, N., Jahangir, K., Shah, S.M., El-Gendy, A.A., 2008. Pharmaceutical significance of cellulose: a review. Express. Polym. Lett. 2 (11), 758–778. https://doi.org/10.3144/expresspolymlett.2008.90.

Kang, Y., Xiong, Y., Lu, B., Wang, Y., Zhang, D., Feng, J., Chen, L., Zhang, Z., 2024. Application of In situ mucoadhesive hydrogel with anti-inflammatory and pro-repairing dual properties for the treatment of chemotherapy-induced oral mucositis. ACS. Appl. Mater. Interfaces. 16 (28), 35949–35963. https://doi.org/10.1021/acsami.4c03217.

Katzung, B.G., 2019. Basic & Clinical Pharmacoloy, 14th Edition. Education, McGraw-Hill.

Korelc, K., Larsen, B.S., Gašperlin, M., Tho, I., 2023. Water-soluble chitosan eases development of mucoadhesive buccal films and wafers for children. Int. J. Pharm. 631, 122544. https://doi.org/10.1016/j.ijpharm.2022.122544.

Kulkarni, U.D., Mahalingam, R., Li, X., Pather, I., Jasti, B., 2011. Effect of experimental temperature on the permeation of model diffusants across porcine buccal mucosa. AAPS. PharmSciTech. 12 (2), 579–586. https://doi.org/10.1208/s12249-011-9624-z.

Lalla, R.V., Sonis, S.T., Peterson, D.E., 2008. Management of oral mucositis in patients who have cancer. Dent. Clin. North Am. 52 (1), 61–77. https://doi.org/10.1016/j.cden.2007.10.002.

Li, T., Bao, Q., Shen, J., Lalla, R.V., Burgess, D.J, 2020. Mucoadhesive in situ forming gel for oral mucositis pain control. Int. J. Pharm. 580, 119238. https://doi.org/10.1016/j.ijpharm.2020.119238.

Luck, P., Vårum, K.M., Foegeding, E.A., 2015. Charge related astringency of chitosans. Food Hydrocoll. 48, 174–178. https://doi.org/10.1016/j.foodhyd.2015.02.024.

Mahadevaiah, Shivakumara, L.R., Demappa, T., Singh, V., 2016. Mechanical and barrier properties of hydroxy propyl methyl cellulose edible polymer films with plasticizer combinations. J. Food Process. Preserv. 41 (4), e13020. https://doi.org/10.1111/jfpp.13020.

Martins, M.L., Eckert, J., Jacobsen, H., Dos Santos, E.C., Ignazzi, R., Araujo, D.R.De, Bellissent-Funel, M.-C., Natali, F., Koza, M.M., Matic, A., De Paula, E., Bordallo, H.N, 2017. Raman and infrared spectroscopies and X-ray diffraction data on bupivacaine and ropivacaine complexed with 2-hydroxypropyl−β−cyclodextrin. Data Br. 15, 25–29. https://doi.org/10.1016/j.dib.2017.08.053.

Mogensen, S., Treldal, C., Sveinsdottir, K., Jensen, K., Kristensen, C.A., Mogensen, T.S., Petersen, J., Andersen, O., 2016. A novel lozenge containing bupivacaine as topical alleviation of oral mucositis pain in patients with head and neck cancer: a pilot study. Pain. Rep. 1 (3), e571. https://doi.org/10.1097/PR9.0000000000000571.

Ngo, A.L., Urits, I., Yilmaz, M., Fortier, L., Anya, A., Oh, J.H., Berger, A.A., Kassem, H., Sanchez, M.G., Kaye, A.D., Urman, R.D., Herron, E.W., Cornett, E.M., Viswanath, O., 2020. Postherpetic neuralgia: current evidence on the topical film-forming spray with bupivacaine hydrochloride and a review of available treatment strategies. Adv. Ther. 37 (5), 2003–2016. https://doi.org/10.1007/s12325-020-01335-9.

Paczkowska-Walendowska, M., Rył, A., Kwiatek, J., Rosiak, N., Szarzyński, K., Wawrzyniak, W., Ziółkowska, J., Kuderska, W., Krecka, K., Marciniak, A., Karpiński, T.M., Plech, T., Miklaszewski, A., Owczarz, P., Cielecka-Piontek, J., 2025. Baicalein-loaded Chitosan films for local treatment of oral infections. Polym 17 (16), 2167. https://doi.org/10.3390/polym17162167.

Patel, V.F., Liu, F., Brown, M.B., 2011. Advances in oral transmucosal drug delivery. J. Control Release 153 (2), 106–116. https://doi.org/10.1016/j.jconrel.2011.01.027.

Preis, M., Woertz, C., Kleinebudde, P., Breitkreutz, J., 2013. Oromucosal film preparations: classification and characterization methods. Expert. Opin. Drug Deliv. 10 (9), 1303–1317. https://doi.org/10.1517/17425247.2013.804058.

Preis, M., Woertz, C., Schneider, K., Kukawka, J., Broscheit, J., Roewer, N., Breitkreutz, J., 2014. Design and evaluation of bilayered buccal film preparations for

local administration of lidocaine hydrochloride. Eur. J. Pharm. Biopharm. 86 (3), 552–561. https://doi.org/10.1016/j.ejpb.2013.12.019.
Reynolds, T.D., Gehrke, S.H., Hussain, A.S., Shenouda, L.S., 1998. Polymer erosion and drug release characterization of hydroxypropyl methylcellulose matrices. J. Pharm. Sci. 87 (9), 1115–1123. https://doi.org/10.1021/js980004q.
Sarvizadeh, M., Hemati, S., Meidani, M., Ashouri, M., Roayaei, M., Shahsanai, A., 2015. Morphine mouthwash for the management of oral mucositis in patients with head and neck cancer. Adv. Biomed. Res. 4, 44. https://doi.org/10.4103/2277-9175.151254.
Shipp, L., Liu, F., Kerai-Varsani, L., Okwuosa, T.C., 2022. Buccal films: a review of therapeutic opportunities, formulations & relevant evaluation approaches. J. Control Release 352, 1071–1092. https://doi.org/10.1016/j.jconrel.2022.10.058.
Sigma-Aldrich. (n.d.). Bupivacaine hydrochloride monohydrate. Retrieved November 14, 2025, from https://www.sigmaaldrich.com/NO/en/substance/bupivacainehydrochloridemonohydrate3429073360540?srsltid=AfmBOorIZfS5daxLexKpAYbWzOfovOqZBm3T8cRSUFiw-H_aY3H6JB6A.
Smart, J.D., 2005. Buccal drug delivery. Expert. Opin. Drug Deliv. 2 (3), 507–517. https://doi.org/10.1517/17425247.2.3.507.
Souza de Freitas Domingues, J., Martins Dias Dos Santos, S., das Neves Rodrigues Ferreira, J., Miguel Monti, B., Favero Baggio, D., Hummig, W., Araya, E.I., de Paula, E., Geremias Chichorro, J., Nunes Ferreira, L.E., 2022. Antinociceptive effects of bupivacaine and its sulfobutylether-β-cyclodextrin inclusion complex in orofacial pain. Naunyn-Schmiedeb. Arch. Pharmacol. 395 (11), 1405–1417. https://doi.org/10.1007/s00210-022-02278-4.
Su, J., Liu, C., Sun, A., Yan, J., Sang, F., Xin, Y., Zhao, Y., Wang, S., Dang, Q., 2025. Hemostatic and antimicrobial properties of chitosan-based wound healing dressings: a review. Int. J. Biol. Macromol. 306 (Part 2), 141570. https://doi.org/10.1016/j.ijbiomac.2025.141570.
Su, X., Yang, Z., Bing, K., Chen, J., Huang, J., Li, Q., 2020. Preparation and characterization of ethyl cellulose film modified with capsaicin. Carbohydr. Polym. 241, 116259. https://doi.org/10.1016/j.carbpol.2020.116259.
Szymańska, E., Winnicka, K., 2015. Stability of Chitosan—A challenge for pharmaceutical and biomedical applications. Mar. Drugs 13 (4), 1819–1846. https://doi.org/10.3390/md13041819.
Tofoli, G.R., Boava Papini, J.Z., Furlan, B., Saia Cereda, C.M., Calafatti, S.A., de Paula, E., Franz-Montan, M., Santi, P., Nicoli, S., Pescina, S., Ribeiro de Araujo, D., Pelosine, A. M., Padula, C., 2025. Bioadhesive film for the delivery of local anesthetics to the buccal mucosa: ex-vivo and in-vivo evaluation. J. Drug Deliv. Sci. Technol. 103, 106446. https://doi.org/10.1016/j.jddst.2024.106446.
Tzanova, M.M., Hagesaether, E., Tho, I., 2021. Solid lipid nanoparticle-loaded mucoadhesive buccal films – Critical quality attributes and in vitro safety & efficacy. Int. J. Pharm. 592, 120100. https://doi.org/10.1016/j.ijpharm.2020.120100.
Wiedmer, S.K., Sohn, J.-T., 2024. Lipophilicity of drugs, including local anesthetics, and its association with lipid emulsion resuscitation. Korean J. Anesth. 77 (1), 170–172. https://doi.org/10.4097/kja.23825.
Younes, I., Rinaudo, M., 2015. Chitin and chitosan preparation from marine sources. Structure, properties and applications. Mar. Drugs 13 (3), 1133–1174. https://doi.org/10.3390/md13031133. *113*(3).